Modeling and control of a floating platform

For the sake of comparison, we have also tried to solve the above problems using the results of [10] where the solvability of the ϵ-scaled $\mathcal{H}_\infty$ problem has been tested by means of the necessary and sufficient conditions provided in [12]. Unfortunately, considering $\gamma \in [52, 60]$ dB and $\epsilon \in [0.1, 1000]$, we were not able to find a pair (γ, ϵ) in such a way the proposed auxiliary "ϵ-scaled" $\mathcal{H}_\infty$ problem (see [10]) could be solvable. In fact, a conclusion can not be drawn since the authors do not provide a procedure for tuning the involved parameters. Taking $\gamma = 52.00$ dB and $\epsilon = 1$, however, the auxiliary "ϵ-scaled" $\mathcal{H}_\infty$ problem turns to be solvable for $a_{12}, b_{22} \in [0.0458, 0.0620]$, yielding

$$K = [10.7270 \quad 9.2274].$$

Note that the above feedback gain assures quadratic stability with γ disturbance attenuation for uncertainties which, compared with (22), represents a reduction of 70% of the uncertain interval, around the same nominal point.

V. Conclusions

This paper addresses $\mathcal{H}_\infty$ control design problems considering parameter uncertainties. The open-loop discrete-time system is supposed to belong to convex-bounded uncertain domains, without any kind of matching conditions. The results follow from a simple sufficient condition, testing whether the $\mathcal{H}_\infty$ norm of the closed-loop system is limited by some prescribed γ attenuation level. As a consequence, the $\mathcal{H}_\infty$ guaranteed cost control problem turns out to be convex, as well as the optimal $\mathcal{H}_\infty$ guaranteed cost control, where γ is involved in the optimization process. The mixed $\mathcal{H}_2/\mathcal{H}_\infty$ guaranteed cost control problem can also be handled by the above convex approach, merely extending the previous results. This approach is compared with others presented in the literature by means of an example, which highlights the advantages of the proposed method.

References

[1] R. T. Bambang, E. Shimemura, and K. Uchida, "Discrete-time $\mathcal{H}_2/\mathcal{H}_\infty$ robust control with state feedback," in *Proc. 1991 Amer. Contr. Conf.*, Boston, MA, 1991, pp. 1172–1173.

[2] J. C. Geromel, P. L. D. Peres, and J. Bernussou, "On a convex parameter space method for linear control design of uncertain systems," *SIAM J. Contr. Optim.*, vol. 29, no. 2, pp. 381–402, Mar. 1991.

[3] J. C. Geromel, P. L. D. Peres, and S. R. de Souza, "$\mathcal{H}_2$ guaranteed cost control for uncertain discrete-time linear systems," *Int. J. Contr.*, vol. 57, no. 4, pp. 853–864, 1993.

[4] P. A. Iglesias and K. Glover, "State space approach to discrete-time $\mathcal{H}_\infty$ control," *Intern. J. Contr.*, vol. 54, no. 5, pp. 1031–1073, 1991.

[5] I. Kaminer, P. P. Khargonekar, and M. A. Rotea, "Mixed $\mathcal{H}_2/\mathcal{H}_\infty$ control for discrete-time systems via convex optimization," in *Proc. 1992 Amer. Contr. Conf.*, Chicago, IL, 1992, pp. 1363–1367.

[6] D. Luenberger, *Linear and Nonlinear Programming*. Reading, MA: Addison-Wesley, 1984.

[7] R. A. Paz and J. V. Medanić, "Robust stabilization and disturbance attenuation for discrete-time systems with structured uncertainty," in *Proc. 1992 Amer. Contr. Conf.*, Chicago, IL, USA, 1992, pp. 2911–2915.

[8] P. L. D. Peres, J. C. Geromel, and S. R. Souza, "Convex analysis of discrete-time uncertain $\mathcal{H}_\infty$ control problems," in *Proc. 30th Conf. Decision Contr.*, vol. 1, Brighton, UK, 1991, pp. 521–526.

[9] P. L. D. Peres and J. C. Geromel, "$\mathcal{H}_2$ control for discrete-time systems: optimality and robustness," *Automatica*, vol. 29, No. 1, pp. 225–228, 1993.

[10] C. E. de Souza, M. Fu, and L. Xie, "$\mathcal{H}_\infty$ analysis and synthesis of discrete-time systems with time-varying uncertainty," *IEEE Trans. Automat. Contr.*, vol. 38, no. 3, pp. 459–462, Mar. 1993.

[11] C. E. de Souza and L. Xie, "On the discrete-time bounded real lemma with application in the characterization of static state feedback $\mathcal{H}_\infty$ controllers," *Syst. Contr. Lett.*, vol. 18, pp. 67–71, 1992.

[12] I. Yaesh and U. Shaked, "A transfer function approach to the problems of discrete-time systems: $\mathcal{H}_\infty$ optimal linear control and filtering," *IEEE Trans. Automat. Contr.*, vol. 36, no. 11, pp. 1264–1271, Nov. 1991.

[13] E. Yaz and R. E. Skelton, "On covariance control for linear discrete-time systems," in *Proc. 1991 Allerton Conf.*, IL, 1991, pp. 717–726.

Modeling and Control of a Floating Platform

Ad A. H. Damen, Heinz M. Falkus, and Jo P. H. M. Bouwels

***Abstract*—A platform with a rotating crane resting on three adjustable floats in a tub has been built on laboratory scale. Controller design is studied to prevent the platform from leaning due to crane movements. The system dynamics can be described primarily by a simple sixth order linear model. Model errors are then due mainly to unmodeled effects of waves that are essentially linear transfers. It is precisely under these conditions that H_∞ design should perform well. Actual design and tests show that H_∞ controllers do not substantially outperform LQG designs combined with feedforward controllers, but the combination of both feedforward and feedback controllers can easily be obtained by H_∞ design techniques.**

I. Introduction

A floating platform with a rotating crane has been built on laboratory scale to evaluate identification and control theories. This particular process was chosen because it is an essentially linear MIMO system. It can be described well by three decoupled, second order SISO (single-input/single-output) systems. The model errors are then mainly caused by unmodeled waves. Although these wave dynamics are essentially linear, they are difficult to model because of changing reflections that lead to time varying delays. The fact that H_∞ control is said to be particularly suited for robust control in cases of unmodeled linear dynamics made this case study an excellent example for testing H_∞ design.

Although the laboratory process has been used to test both system identification and control design, the system identification phase has been skipped here and only a short process description extended with modeling considerations is given. The main focus is on H_∞ control compared to LQG and feedforward control where all controllers are designed to reduce the leaning of the platform caused by crane movements and other disturbances.

II. Process Description, Modeling and Identification

The platform, weighing about 20 kg, with vertically movable floats has been positioned in a water tub of about two m diameter as shown in Fig. 1. The actual platform is mounted on three horizontal beams connected at angles of 120° with their ends resting on vertical steel

Manuscript received September 25, 1992; revised February 17, 1993.

A. A. H. Damen and H. Falkus are with the Measurement and Control Group of the Department of Electrical Engineering, Eindhoven University of Technology, The Netherlands.

J. Bouwels is with Siemens Nederland N.V., Department EV (Energy Supplies), Den Haag, The Netherlands.

IEEE Log Number 9400345.

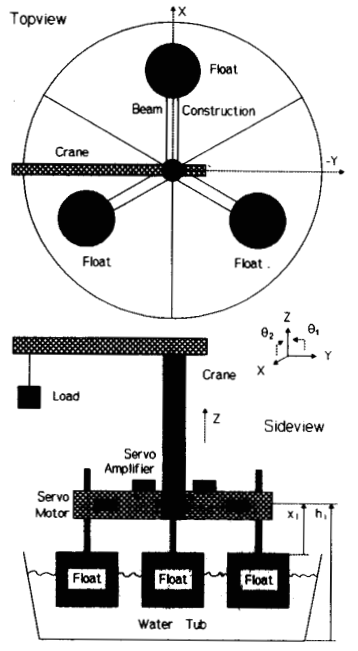

Fig. 1. The floating platform.

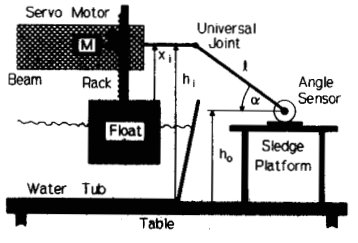

Fig. 2. Actuator and sensor construction.

rods with racks. These rods are elevated by floats and the distance x_i of the floats to the platform can be controlled on each beam by servo-motors, as shown in Fig. 2. The height h_i from the end of beam i to the ground level has been measured by an angle sensor mounted on a sledge that can freely slide on a fixed platform of height h_0. The axle of the angle sensor is connected with a rod via a universal joint to the end of the beam so that: $h_i = l \sin(\alpha) + h_0$.

A crane driven by a servo-motor and rotating a load of one kg has been mounted on the platform. This causes the platform to tilt. The control to be designed should prevent this tilting.

In a first approximation, the following description of the system dynamics can be given. Let F_i denote the vertical force of float i applied to the end of beam i. For a small degree of leaning of the platform, these forces will result in a vertical movement h of the gravity center and two rotations θ_y around the negative y-axis and θ_x around the x-axis (the orientation is shown in Fig. 1) according to

$$M\ddot{h} = F_1 + F_2 + F_3 - Mg \qquad h = \frac{1}{3}(h_1 + h_2 + h_3)$$

$$J_y\ddot{\theta}_y = LF_1 - \frac{L}{2}F_2 - \frac{L}{2}F_3 \qquad \theta_y = \frac{2}{3L}\left(h_1 - \frac{1}{2}h_2 - \frac{1}{3}h_3\right) \quad (1)$$

$$J_x\ddot{\theta}_x = \frac{L}{2}\sqrt{3}F_2 - \frac{L}{2}\sqrt{3}F_3 \qquad \theta_x = \frac{\sqrt{3}}{3L}(h_2 - h_3)$$

where M is the total mass, g the gravity acceleration, J_x and J_y the inertia of the x and y rotation, respectively, and L the length of a supporting beam. If we start from a horizontal equilibrium and define this as the working point, we can skip the term $-$Mg and proceed if we take h_i and F_i to be the value with respect to the equilibrium. Ignoring waves, the floats in the water act as springs so that

$$F_i = D(\dot{x}_i - \dot{h}_i) + K(x_i - h_i) \quad (2)$$

where D indicates the damping, K the spring constant, and x_i the distance of float i to the platform defined zero for the equilibrium. The transfer between input v_i of servo-amplifier i to the position x_i around equilibrium can be taken as C/s because the time constants in the servo-system are far less than those of the platform and because overdimensioned servo-motors and a spiral gear justify the neglect of the float movement load on the torque of the servo motor.

Next we define as outputs y_i and inputs u_i of the system

$$y_1 = h_1 + h_2 + h_3 \qquad u_1 = v_1 + v_2 + v_3$$

$$y_2 = h_1 - \frac{1}{2}h_2 - \frac{1}{2}h_3 \qquad u_2 = v_1 - \frac{1}{2}v_2 - \frac{1}{2}v_3 \quad (3)$$

$$y_3 = h_2 - h_3 \qquad u_3 = v_2 - v_3$$

where v_i are the actual inputs to the servo-system, which can easily be computed from u_i. As we were very keen to keep the servo-systems and the float systems exactly the same (so D, K, C), combination of (1), (2) and (3) leads to the following transfer in the Laplace domain

$$\begin{pmatrix} y_1 \\ y_2 \\ y_3 \end{pmatrix} = \begin{pmatrix} P_h(s) & 0 & 0 \\ 0 & P_x(s) & 0 \\ 0 & 0 & P_y(s) \end{pmatrix} \begin{pmatrix} u_1 \\ u_2 \\ u_3 \end{pmatrix} = P(s) \begin{pmatrix} u_1 \\ u_2 \\ u_3 \end{pmatrix} \quad (4)$$

$$P_j(s) = \frac{K_{pj}(sD + K)}{s^2 + K_{pj}(sD + K)} \frac{C}{s}, \qquad K_{ph} = \frac{3}{M},$$

$$K_{px} = \frac{3L^2}{2J_x}, \qquad K_{py} = \frac{3L^2}{2J_y}.$$

So the system appears to be decoupled in a first approximation.

The angle of the crane to the positive y-axis in a clockwise sense from the top view is defined as angle ϕ. In our experiments we simply rotate the crane with a load of mass m (= 1 kg) at the end with a constant rotation speed ω_0 (= 0.251 rad/s). If we neglect the influence of the crane position on the inertia, we only have to deal with a vector of disturbing forces: $\underline{d} = [-mg - mgL\cos(\omega_0 t) - mgL\sin(\omega_0 t)]^T$ added to the left-hand equations of (1). This finally leads to known output disturbances $\underline{d}_r$ by transfer $R(s)$

$$R_j(s) = \frac{K_{rj}}{s^2 + K_{pj}(sD + K)}, \qquad K_{rh} = \frac{3}{M},$$

$$K_{rx} = \frac{2}{\sqrt{3}}\frac{3L^2}{2J_x}, \qquad K_{ry} = \frac{3L^2}{2J_y}$$

and K_{pj} as in (4).

$$\begin{pmatrix} d_{r1} \\ d_{r2} \\ d_{r3} \end{pmatrix} = \begin{pmatrix} R_h(s) & 0 & 0 \\ 0 & R_x(s) & 0 \\ 0 & 0 & R_y(s) \end{pmatrix} \begin{pmatrix} -\frac{mg}{s} \\ -\frac{mgs}{s^2+\omega_0^2} \\ -\frac{mg\omega_0}{s^2+\omega_0^2} \end{pmatrix} = R(s) \begin{pmatrix} d_1 \\ d_2 \\ d_3 \end{pmatrix} \quad (5)$$

System identification shows that the unmodeled dynamics are mainly due to the waves in the water rebounding against the floats and the wall of the tub. This influences the lift of the floats. These wave effects can be represented by linear transfers but, as the platform drifts and rotates slightly in the tub, the transfers change slowly in time, making simple time invariant low order modeling impossible.

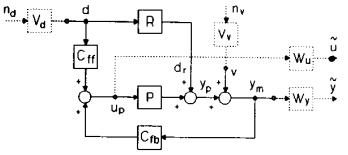

Fig. 3. Controlled system configuration.

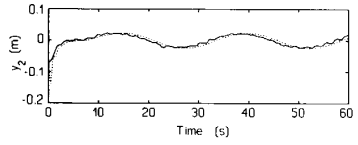

Fig. 4. Measured (solid) and simulated (dashed) rotation around x-axis with LQG control.

After establishing the main dynamics in the qualitative transfer of (4), the quantitative transfer was identified in discrete-time domain, according to the method in [1]. Preliminary measurements according to [2] indicated a sampling frequency of 10 Hz, while the resonance frequencies were around 1.5 Hz.

The final model resulting from identification takes the form of three second-order SISO systems extended with an integration as in (4). The representation is in state space where the states are the (angle) position x_1, (rotation) speed x_2 and (rotation) acceleration x_3.

For the controller design each pair of SISO transfers P_j and R_j is treated separately and their subscripts and those of u_i, d_i, and y_i are omitted unless specific examples are given.

III. LQG and Feedforward Control

For each P (actually P_j) of (4) an observer has been constructed obtaining the Kalman gains by minimizing the summed squares of the innovations $e(k) = y(k) - \hat{y}(k)$, where $\hat{y}(k)$ is the output of the observer for a Gaussian white noise input u. The estimated innovations have been tested on their whiteness by means of their auto-correlation. The slight nonwhiteness left is due to remaining wave effects. Nevertheless, we may represent a substantial part of the disturbances, such as drift in the servo-amplifier and the waves in the tub, by the innovations and the innovation filter such that

$$y(k) = H(zI - F)^{-1}Gu(k) + \frac{|zI - F + QH|}{|zI - F|}e(k) \qquad (6)$$

where $\{F, G, H\}$ represents the realization of the process P under study in (4) and Q is the obtained Kalman gain.

Next, a linear state controller has been designed by minimizing $E\{100x_1^2+x_2^2+x_3^2+u^2\}$. Increasing the weight 100 on the (position) state x caused instability for the real process, due to the unmodeled waves so that the obtainable band for disturbance reduction is limited. It was not necessary to penalize variations of speed and acceleration so that their weights are kept on value one. This controller combined with the observer is represented by C_{fb} in Fig. 3. An example of the obtained performance is shown in Fig. 4. The plant and the controller are switched on at $t = 0s$, and at $t = 7s$ the crane starts rotating. Without a controller, the amplitude of the sinusoid is about 0.06 m so that a reduction factor of three is obtained by this control.

Since the disturbance d of the rotating crane can be measured and the transfer R of this disturbance to the actual output has been modeled, it is theoretically possible to compute a feedforward controller for the improvement in the higher frequencies by $C_{ff} = -RP^{-1}$ as shown in Fig. 3, thereby annihilating the d_r at the output.

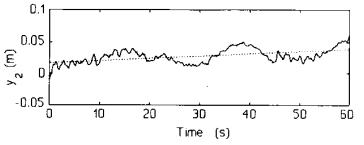

Fig. 5. Measured (solid) rotation around x-axis with feedforward control (dashed line = drift).

Therefore we have to invert the transfer P, which seems to cause no problems as this transfer is minimum phase and P and R share the same poles. The integration in P, however, leads to a differentiation within C_{ff}, and consequently, it is not possible to correct for the effects of the very low frequencies present in the disturbances. This can be observed in Fig. 5, showing a clear drift, when feedforward is exclusively applied. Nevertheless, the feedforward control has advantages in the high frequency band, where LQG fails because too much feedback in this band causes instability. A combination of both would therefore be beneficial, and this has been realized in the next H_∞ control design.

IV. H_∞ Control

For the H_∞ design we used the configuration of Fig. 3 leading to a two-degree-of-freedom controller combining C_{ff} and C_{fb}.

The filter V_d is used to characterize the crane disturbance, where the disturbance signals are: $d_h(k) = -mg\,\epsilon(k), d_x(k) = -mg \sin(\omega_0 kT_s)$, and $d_y(k) = -mg\cos(\omega_0 kT_s)$ with ϵ a step disturbance of the average height. The z-transforms of these signals could be used directly as the filter(s) V_d (for each SISO subsystem), but to ensure that the system will also be robust for small variations of the load and the rotation frequency around their nominal value, a damping factor ($\beta = 0.025$) has been included.

The disturbances, such as drift in servo-amplifiers and unmodeled waves, are represented by n_v and filter V_v. In (6) these disturbances are represented by the second term and correspondingly we define V_v by $|zI - F + QH|/|zI - F|$.

The weight W_u is designed to avoid saturation of the servo-amplifier. Because this saturation is mainly caused by peaks in the control signal, W_u has to be high pass. Weight W_y determines the band for which there should be substantial reduction of the disturbances. Therefore W_y is a low pass filter. The controller optimization is done by modifying the gains, the cross-over frequencies and the slopes of these filters W_u and W_y with fixed filters V_v and V_d until satisfactory control results: i.e., a maximum disturbance reduction under the constraint of stability and no actuator saturation, both validated in practice. In each iteration the H_∞ controllers are found by minimization under stability constraint of

$$\min_{C_{fb}, C_{ff}} \|G\|_\infty = \gamma. \qquad (7)$$

The entries of the generalized transfer G from n_v, n_d to $\tilde{y}$, $\tilde{u}$ are represented in Table I. For the repeated computation of the controllers with changing weighting filters the program package designed by Falkus [3] was used.

The robustness for modeling errors can be interpreted as follows. Since integration is part of the transfer of the plant, one can best account for the modeling errors using stable factor perturbation so that the real transfer becomes

$$\tilde{P} = (M + \Delta M)^{-1}(N + \Delta N) \qquad (8)$$

where the nominal model is given by $P = M^{-1}N$. According to McFarlane [4], stability is guaranteed if C_{fb} stabilizes the nominal

TABLE I
ENTRIES OF GENERALIZED TRANSFER G.

Subcriterion	Description	Weight	Transfer
$G_{11} = \tilde{y}/n_v$	Sensitivity	$W_y V_v$	$(I - PC_{fb})^{-1}$
$G_{12} = \tilde{y}/n_d$	(Disturbance reduction)	$W_y V_d$	$(I - PC_{fb})^{-1}(R + PC_{ff})$
$G_{21} = \tilde{u}/n_v$	Control sensitivity	$W_u V_v$	$C_{fb}(I - PC_{fb})^{-1}$
$G_{22} = \tilde{u}/n_d$	(Actuator saturation)	$W_u V_d$	$(I - PC_{fb})^{-1}(C_{fb}R + C_{ff})$

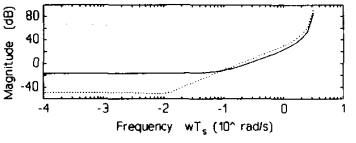

Fig. 6. Weighting filters: W_{uh} (solid), $W_{ux} = W_{uy}$ (dashed) and $W_{yh} = W_{yx} = W_{yy}$ (dotted).

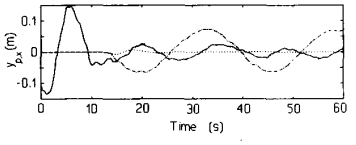

Fig. 7. Rotation around x-axis; Measured (solid) and simulated (dashed) with control, measured (dash-dot) and simulated (dotted) without control.

plant and

$$\left\| \begin{matrix} W_M(I - PC_{fb})^{-1}M^{-1} \\ W_N C_{fb}(I - PC_{fb})^{-1}M^{-1} \end{matrix} \right\|_\infty \leq \epsilon$$
$$\text{while} \quad \left\| \Delta M W_M^{-1} \quad \Delta N W_N^{-1} \right\|_\infty < \epsilon^{-1}. \tag{9}$$

Since V_v contains the poles of the transfer P including the integration, we can take $M^{-1} = V_v$ (see also [5]), thereby implicitly defining $N = V_v^{-1}P$. The condition (9) is then incorporated in G_{11} and G_{21} for $W_M = W_y$ and $W_N = W_u$ and ϵ bounded by γ.

The optimized filters W_u and W_y are depicted in Fig. 6. The three sub-processes as well as the corresponding design filters are quite similar. Due to this we obtain almost the same closed-loop behavior. Therefore, and because of limited space, we again only show the results for the rotation around the x-axis with $\gamma_x = 1.6925$ in Fig. 7. The behavior in the first 13.5 seconds is caused by starting up the system. After 13.5 seconds, the crane starts rotating. If we try to improve the disturbance rejection, the system becomes unstable in practice. Apparently the H_∞ norm then becomes too large, i.e., $\gamma_x > 1.6925$, implying too little robustness against modeling errors mainly due to wave effects. It is difficult to model the wave effects because of the multiple reflections against the tub wall and other floats. So simply increasing the model order would not solve this problem. As an alternative, we plan to measure the wave effects using special sensors around the floats and add these measurements as extra inputs to the controller. These sensors are included in a new platform design that is currently being built.

V. CONCLUSIONS

For a laboratory plant we derived a simple model describing the response to servo-control input. The effects of crane movements that can be measured have also been modeled. A simple innovations representation has been estimated to represent disturbances such as drift in servo amplifiers and waves in the tub.

Based upon this information, we designed controllers according to LQG, feedforward, and H_∞ concepts. We tried to obtain a disturbance rejection for a frequency band as broad as possible until instability or actuator saturation occurred. It was then observed that the H_∞ design, along the lines presented, did not perform substantially better than controllers from LQG and feedforward design.

REFERENCES

[1] A. C. P. M. Backx and A. A. H. Damen, "Identification for the control of MIMO industrial processes," *IEEE Trans. Automat. Contr.*, vol. 37, no. 7, pp. 980–986, 1992.

[2] ——, "Identification of MIMO industrial processes for fixed controllers, Part 1: General theory and practice," *J. A*, vol. 30, no. 1, pp. 3–12; "Part 2: Case studies," *J. A*, vol. 30, no. 2, pp. 33–43, 1989.

[3] H. M. Falkus, A. A. H. Damen, and J. Bouwels, "General MIMO H_∞ control design framework," in *Proc. 31st Conf. Decision Contr.*, 1992, pp. 2181–2186.

[4] D. C. McFarlane and K. Glover, "Robust controller design using normalized coprime factor plant descriptions," in *Lecture Notes in Control and Information Sciences*, no. 138. New York: Springer-Verlag, 1990.

[5] M. Klompstra, A. J. J. v.d. Boom, and A. A. H. Damen, "A comparison of classical and modern controller design: A case study," EUT Rep. 90-E-244, Dept. electrical engineering, Eindhoven Univ. Tech., The Netherlands, 1990.